

# Deuteron Electro-Disintegration At Very High Missing Momenta

Carlos Yero

February 19, 2017

A research proposal presented for the degree of  
Doctor of Philosophy in Physics



Department of Physics  
Florida International University, Miami FL  
USA

# 1 Motivation

The deuteron ( ${}^2\text{H}$ ) was discovered in 1931 by Harold Urey, and it remained a mystery until the discovery of the neutron by James Chadwick the following year [9]. Since then, the deuteron has been under intensive research in an attempt to understand what binds the atomic nucleus. Being a simple  $np$  bound state, the deuteron serves as a starting point to study the strong nuclear force at the sub-fermi level which is currently not well understood. At such small internucleon distances the NN (nucleon-nucleon) potential is expected to exhibit a repulsive core in which the interacting nucleon pair begins to overlap. The overlap is directly related to two-nucleon short range correlations (SRC) observed in  $A \geq 2$  nuclei [8]. Short-distance studies of the deuteron are also important in determining whether or to what extent the description of nuclei in terms of nucleon/meson degrees of freedom must be supplemented by the inclusion of explicit quark effects [10].

In nuclear structure studies in general, electron-nucleon scattering serves as the most valuable tool since the interaction is described by Quantum Electro-Dynamics (QED), which is well-understood and capable of making accurate predictions. Electron scattering experiments can be separated into inclusive or exclusive scattering experiments. In the first of these, only the electron is detected in the final state (single-arm experiments), and so one studies the nucleus in question by integrating over all possible final states [1]. In the exclusive type, one or more particles are detected in coincidence with the scattered electron which allows one to investigate properties unique to the specific reaction in question. In deuteron electro-disintegration, for example, one detects the scattered electron in coincidence with a proton and the missing neutron is reconstructed from four-momentum conservation. This reaction proves to be the most direct way of probing the internal structure of the deuteron since it is possible to deduce the internal momentum of the nucleons from the neutron missing momentum.

With the 12 GeV Upgrade at Jefferson Lab, the short-range ( $\leq 1$  fm) structure of the deuteron will become experimentally accessible via data on the deuteron wavefunction beyond relative internal momenta of 400 MeV/c. At such high energies, one will be able to probe if effects due to Quantum Chromodynamics (QCD) start playing a more significant role [8].

## 2 Theoretical Framework of D(e,e'p)n

Deuteron electro-disintegration can be pictorially described by a Feynmann diagram (See Figure 1) where the

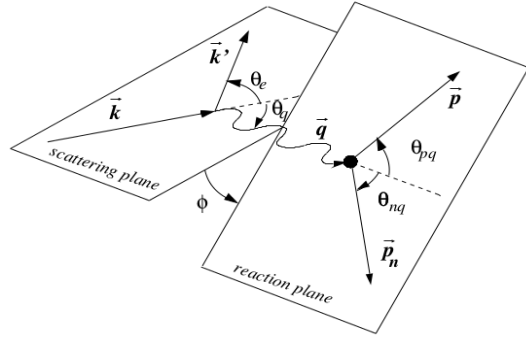


**Figure 1:** Feynmann diagram of deuteron electro-disintegration

incoming electron interacts with the stationary deuteron to first order approximation via the exchange of a virtual photon. Given the relatively weak coupling constant for this process, higher order Feynmann diagrams involving multiple photon exchanges may be neglected. The interaction of the virtual photon with the deuteron is best described by the general unpolarized  $(e, e' p)$  cross section,[1]

$$\frac{d^6\sigma}{d\omega d\Omega_e dT_p d\Omega_p} = \sigma_{Mott}(v_L R_L + v_T R_T + v_{LT} R_{LT} \cos \phi + v_{TT} R_{TT} \cos 2\phi) \quad (1)$$

where  $\sigma_{Mott}$  is the Mott cross section describing electron scattering off an infinitely massive, spinless point charge. The quantities  $(v_i, v_{ij})$  are dependent on electron kinematics (i.e.,  $q, Q^2, \theta_e$ ) and the functions  $(R_i, R_{ij})$  are nuclear response functions and depend on nuclear charge and current density operators [5].

In the simplest approximation, the virtual photon couples to the proton which is ejected from the nucleus without further interaction with the recoiling nucleus which carries a momentum  $\mathbf{p}_m = -\mathbf{p}_{i,p}$ . Both final state proton and neutron are assumed to be plane waves (free particles), hence the name Plane Wave Impulse Approximation (PWIA). (See Figure 2)

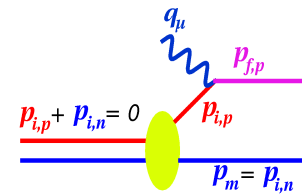


**Figure 2:** Feynmann diagram for PWIA, where the proton(red) is knocked by the photon, and the neutron(blue) scatters as a spectator

From the PWIA assumptions, the general  $(e, e' p)$  cross section (See Eq.1) can be factorized into

$$\sigma_{exp} \equiv \frac{d^6\sigma}{d\omega d\Omega_e dT_p d\Omega_p} = K \sigma_{ep} S(E_m, p_m) \quad (2)$$

where  $K$  is a kinematic factor,  $\sigma_{ep}$  describes the elementary electron-proton cross section for electron scattering off a bound proton, and  $S(E_m, p_m)$  is a spectral function which can be interpreted as the probability of finding a recoiling nucleon with missing energy and momentum [5].

In reality, the final state particles undergo subsequent interactions resulting in re-scattering of the proton and neutron. This process is known as Final State Interactions (FSI) (See Figure 3) and has been shown to have a significant contribution to the experimental cross section at high missing momenta (See Figure 7), therefore one cannot be confident that at large missing momenta, the high momentum component of the deuteron will be probed [2].

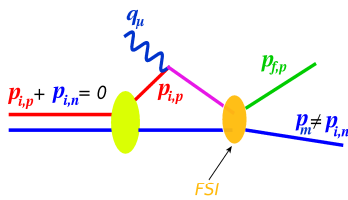


**Figure 3:** Feynmann diagram for FSI, where the proton(red), after excitation by the photon, undergoes subsequent interactions (orange) with the neutron(blue) resulting in a re-scattering of both final state particles.

Another possibility is that the photon may couple to the virtual meson being exchanged between the nucleons (Meson Exchange Currents or MEC). (See Figure 4)

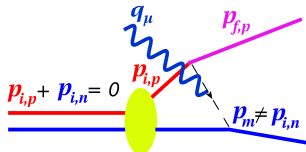


**Figure 4:** Feynmann diagram for MEC, where the virtual photon couples to the exchange meson (dashed line) causing the spectator neutron(blue) to re-scatter off the proton(red)

Or, the photon may excite either nucleon in the deuteron (Isobaric Configuration or IC). (See Figure 5)

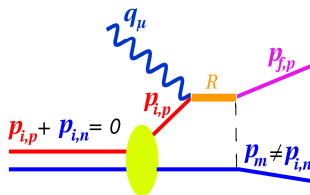


**Figure 5:** Feynmann diagram for IC, where the proton(red) is excited by the photon into an intermediate state (orange) R. The excited state decays and rescatters off the neutron(blue) in the process

It is possible to extract the reduced cross section  $\sigma_{red}$  by dividing Eq. 2 by  $K$  and  $\sigma_{ep}$  and integrating over the

missing energy to obtain

$$\sigma_{red} \equiv S(p_m) = \frac{\sigma_{exp}}{K\sigma_{ep}} \quad (3)$$

If the PWIA were valid, the reduced cross section would be the momentum distribution inside the deuteron, therefore it is important to study at which kinematic settings competing processes are suppressed (MEC, IC), or at least under control (FSI) [8].

FSI are well described by the Generalized Eikonal Approximation (GEA) in the high energy limit ( $Q^2 \geq 1$  (GeV/c) $^2$ ). The GEA predicts a strong angular dependence of FSI as a function of the scattering angle  $\theta_{nq}$  between spectator nucleon and virtual photon, which opens a kinematic window at which FSI are reduced [9]. (See Figure 6)

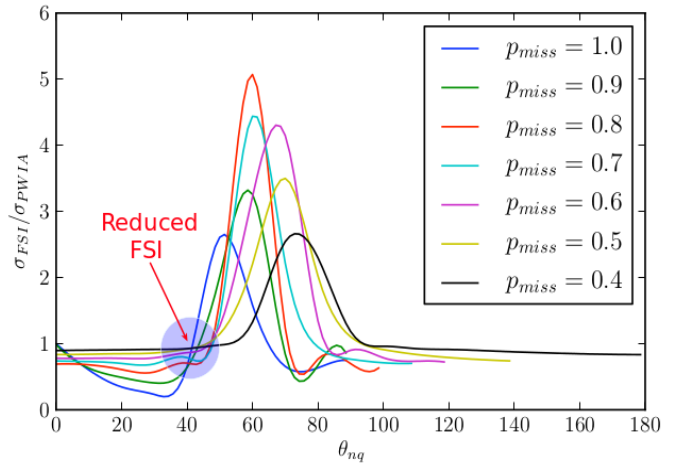


**Figure 6:** Ratio of FSI/PWIA cross-section vs. scattering angle between spectator neutron and virtual photon,  $\theta_{nq}$ , for various missing momenta up to 1 GeV/c [9].

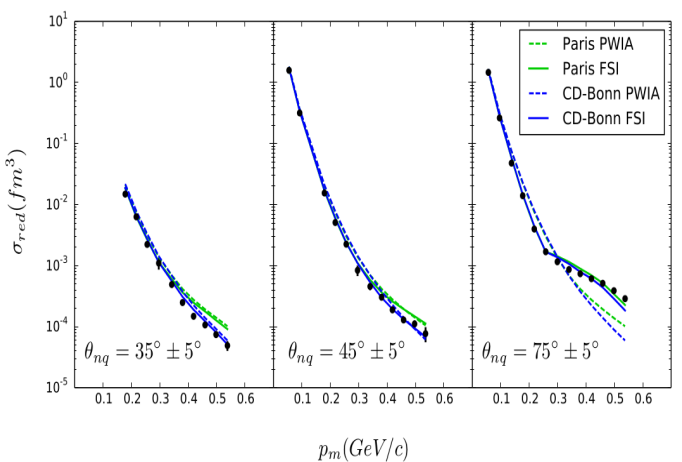


**Figure 7:** Reduced cross-section  $\sigma_{red}$  vs. missing momenta  $p_m$  for angles (a)  $\theta_{nq} = 35^\circ$ , (b)  $\theta_{nq} = 45^\circ$  and (c)  $\theta_{nq} = 75^\circ$  [7].

A previous Hall A experiment (E01-020) [7] at  $Q^2 = 3.5$  (GeV/c)<sup>2</sup> and various  $\theta_{nq}$  examined the effect of FSI for missing momenta up to 0.55 GeV/c. The experiment verified the strong anisotropy of FSI as predicted by GEA. Furthermore, there was shown to be a good agreement between data and theory for reduced cross sections at large missing momenta ( $\geq 300$  MeV/c) for smaller  $\theta_{nq}$  angles without the inclusion of FSI. (See Figure 7 (a) and (b))

### 3 Experimental Hall C Overview

Hall C is one of four experimental halls, each with its unique characteristics for performing a variety of nuclear/particle physics experiments. Hall C in particular has two spectrometers, the High Momentum Spectrometer (HMS) and recently commissioned Super HMS (SHMS), as part of the 12 GeV Upgrade at Hall C. Each spectrometer is comprised of a series of magnets followed by the detector stack (See Figure 8). The magnets are set for a point-to-point tune and transport (focus) the scattered particles to the detectors. The detectors are then read out by Analog- and Time- to Digital Convertors (ADC/TDC)(See p.281 of [6]). To extract meaningful information from the

must be taken into consideration. In E12-10-003 (See Section 4), since a 10-cm long liquid deuterium target ( $T_{\text{freezing}} = 18.7$  K,  $T_{\text{boiling}} = 25.3$  K) needs to be cooled to 22 K, the power delivered by the beam can cause local density fluctuations (local boiling) within the target, and so one needs to study the density fluctuations as a function of beam current in order to correct for target boiling effects [2].

### 4 D(e,e'p)n Commissioning at Hall C

My proposed thesis subject, the Deuteron Electro-Disintegration at Very High Missing Momenta experiment (E12-10-003) will be one of several commissioning experiments scheduled to run on Fall 2017 in Hall C at Jefferson Lab[3]. The experiment will extend the the missing momentum range studied in E01-020 beyond  $p_m = 0.5$  GeV/c at a  $Q^2 = 4.25$  (GeV/c)<sup>2</sup> and  $x_{Bj}=1.35$  for  $\theta_{nq} \sim 40^\circ$  where FSI are expected to be reduced. (See Figure 6)

The main focus of my thesis project will be to extract the unpolarized D(e,e'p)n cross section and momentum distribution for unexplored large missing momentum regions at high  $Q^2$ . The experiment will run at electron beam energy  $E_{beam} = 10.6$  GeV and beam current  $I_b = 70\mu A$ . The missing momentum and spectrometer settings are described in Table 1.

| Kinematic Settings       | HMS                 | SHMS      |
|--------------------------|---------------------|-----------|
| Particles                | protons             | electrons |
| Angle (deg)              | 53.25, 56.40, 59.38 | 12.17     |
| Central Momentum (GeV/c) | 2.30, 2.22, 2.12    | 8.92      |
| Missing Momentum (GeV/c) | 0.50, 0.65, 0.80    |           |

**Table 1:** Kinematic settings for E12-10-003.

In addition to the missing momentum settings explored in E12-10-003, a calibration run will also be taken with the same  $Q^2$  at  $p_{miss} = 80$  MeV/c and  $x_{Bj} = 1.05$  for  $\theta_{nq} \sim 59^\circ$ . The settings for the calibration run are described in Table 2.

| Calibration Settings     | HMS     | SHMS      |
|--------------------------|---------|-----------|
| Particles                | protons | electrons |
| Angle (deg)              | 39.14   | 12.51     |
| Central Momentum (GeV/c) | 2.94    | 8.44      |
| Missing Momentum (GeV/c) | 0.08    |           |

**Table 2:** Calibration settings for E12-10-003.

The commissioning part of E12-10-003 will be given 3 days of beam time. Therefore, it is important to consider the effect of limited statistics on the D(e,e'p)n cross section and how does it compare to the systematic uncertainties given the limited amount of beam time.

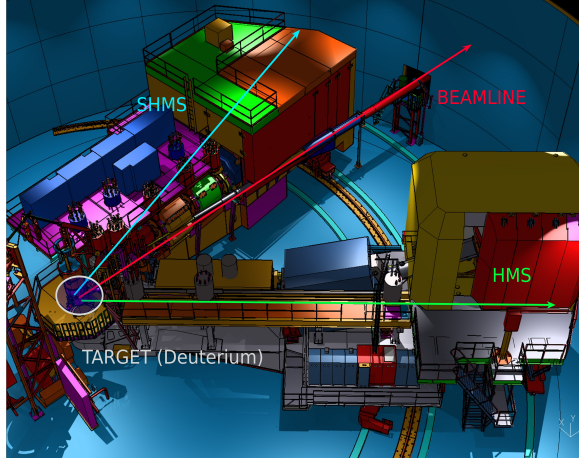


**Figure 8:** Artist view of Hall C HMS/SHMS

underlying physics, magnets and detectors (Hodoscopes, Wire Chambers, Čerenkovs and Calorimeters) must be properly calibrated.

The magnetic optics calibration main objective is to determine the transport matrix elements relating the particle coordinates measured in the focal plane to those in the reaction vertex in the target. Knowledge of the matrix elements will provide a one-to-one mapping of measured particle tracks to the specific target location where the particle originated.

In addition to optics and detector calibrations, Beam Current Monitoring (BCM) and Target Boiling studies

The statistical uncertainties on the D(e,e'p)n cross section were estimated using the standard Hall C simulation program (SIMC) for coincidence reactions. The results are shown in Figures 9 and 10.

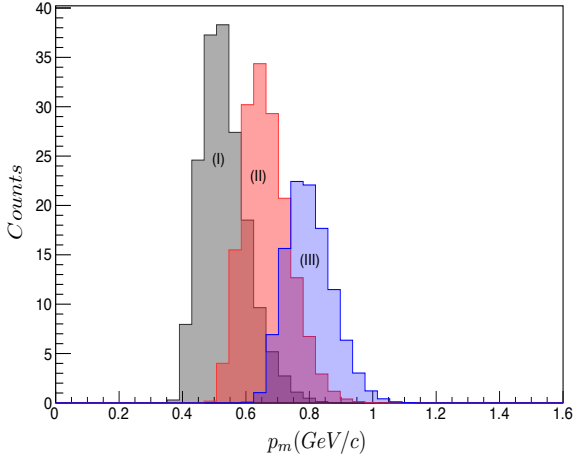


**Figure 9:** Expected (radiative corrected) missing momentum yield after being weighted, for settings and beam time: (I) 0.5 GeV/c (8 hrs), (II) 0.65 GeV/c (18 hrs) and (III) 0.8 GeV/c (36 hrs)

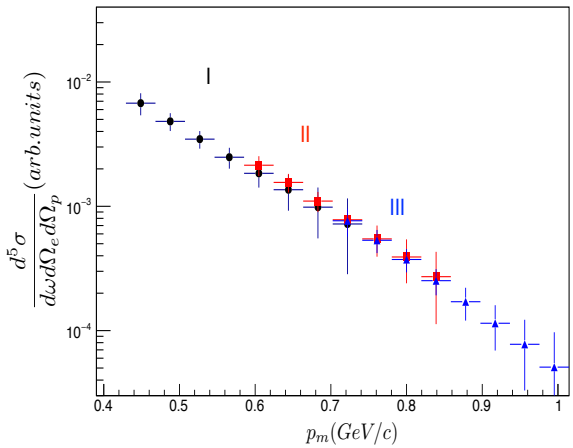


**Figure 10:** The expected D(e,e'p)n cross section results for  $p_{miss} = 0.5, 0.65$  and  $0.8 \text{ GeV}/c$ .

The expected yield in Figure 9 shows an overlap of the three momentum settings to be explored, which can be used to obtain a continuous data set that ranges from  $p_{miss} = 0.5$  to  $1.0 \text{ GeV}$ . The expected cross section, which also shows an overlap of the simulated data points, was calculated by taking the ratio of the weighted yield to the unweighted yield (weight=1). The weight was applied on an event by event basis, and is defined as the product of the luminosity and the cross section. The unweighted yield was determined by Monte Carlo generated events over phase space. The estimated statistical uncertainties for each momentum setting are shown in Table 3.

| Missing Momentum (GeV/c) | Beam Time (hrs) | Statistical Uncertainties (%) |
|--------------------------|-----------------|-------------------------------|
| 0.5                      | 8               | 16.1                          |
| 0.65                     | 18              | 17.0                          |
| 0.8                      | 36              | 20.9                          |

**Table 3:** Statistical uncertainties for each missing momentum setting using SIMC.

In order to understand the effects of systematic uncertainties on the D(e,e'p)n cross section, one needs to investigate how sensitive is the cross section to small variations in measured quantities such as beam energy and spectrometer central momentum and angle settings. These variables and their associated uncertainties are described in Table 4.

| Kinematic Variable                | Symbol                     | Conservative Kinematic Uncertainty | Optimum Kinematic Uncertainty |
|-----------------------------------|----------------------------|------------------------------------|-------------------------------|
| Beam Energy, $E_B$                | $\Delta E_B/E$             | $1 \times 10^{-3}$                 | $5 \times 10^{-4}$            |
| Electron Final Momentum, $k_f$    | $\Delta k_f/k_f$           | $1 \times 10^{-3}$                 | $5 \times 10^{-4}$            |
| Proton Final Momentum, $p_f$      | $\Delta p_f/p_f$           | $1 \times 10^{-3}$                 | $5 \times 10^{-4}$            |
| Electron Scatt. Angle, $\theta_e$ | $\Delta \theta_e/\theta_e$ | $\pm 1\text{mrad}$                 | $\pm 0.2\text{mrad}$          |
| Proton Scatt. Angle, $\theta_p$   | $\Delta \theta_p/\theta_p$ | $\pm 1\text{mrad}$                 | $\pm 0.2\text{mrad}$          |

**Table 4:** Relative uncertainties on kinematic variables[4].

Due to our limited knowledge in some of the spectrometer parameters at this early stage, conservative estimates on various kinematic quantities were made. These estimates were used to determine the systematic error contribution from each of the kinematic variables to the cross section. The results are shown in Table 5 for a range of missing momenta about central setting  $p_{miss} = 0.8 \text{ GeV}/c$ .

| $p_{miss}$ (GeV/c) | Total Error in $d\sigma/d\Omega$ (%) | $\delta E_B$ (%) | $\delta k_f$ (%) | $\delta \theta_e$ (%) | $\delta \theta_p$ (%) |
|--------------------|--------------------------------------|------------------|------------------|-----------------------|-----------------------|
| 0.69               | 7.4                                  | 1.1              | 0.6              | 7.0                   | 2.2                   |
| 0.72               | 7.6                                  | 1.2              | 0.7              | 7.1                   | 2.3                   |
| 0.76               | 7.8                                  | 1.2              | 0.8              | 7.2                   | 2.5                   |
| 0.80               | 8.1                                  | 1.3              | 0.9              | 7.5                   | 2.7                   |
| 0.84               | 8.5                                  | 1.3              | 1.0              | 7.8                   | 2.9                   |
| 0.88               | 9.0                                  | 1.4              | 1.1              | 8.2                   | 3.1                   |
| 0.91               | 9.5                                  | 1.5              | 1.2              | 8.6                   | 3.4                   |
| 0.95               | 10.2                                 | 1.6              | 1.3              | 9.2                   | 3.7                   |
| 0.99               | 11.2                                 | 1.8              | 1.4              | 10.0                  | 4.1                   |

**Table 5:** Systematic errors in the cross section from kinematic variable variations.

Similar results are found for lower missing momentum settings. It is evident from Table 5 that the major contributor to the total systematic error in the cross section is the electron scattering angle,  $\theta_e$ , due to the inverse  $\sin^4 \frac{\theta_e}{2}$  dependence on the cross section.

The systematic and statistical uncertainty contributions to the D(e,e'p)n cross section were estimated and the results are shown in Figure 11.

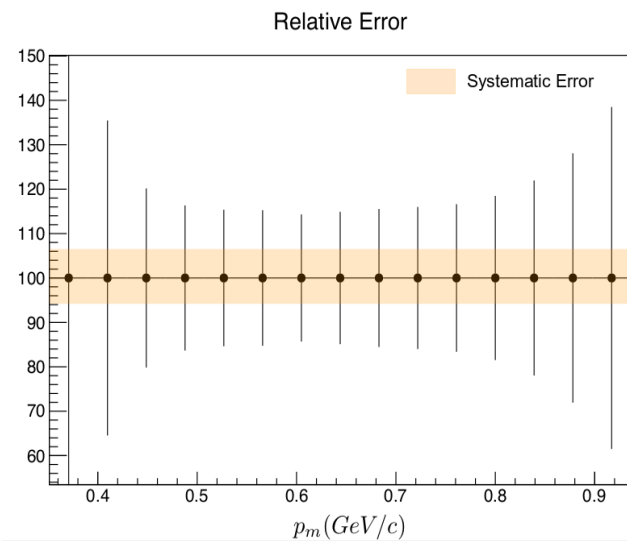


**Figure 11:** Relative error (percent) in the D(e,e'p)n cross section from systematics and statistical contributions for missing momenta up to 1 GeV/c.

It is clear from the range of missing momentum being investigated that the systematics stay well below statistical uncertainties with a maximum systematic error of  $\sim 8\%$ , as compared with a statistical error of  $\sim 16$  to  $21\%$ . This results indicate that the total uncertainty of the cross section can be improved by extending the run period for E12-10-003 after the commissioning part is done.

Studies about the spectrometers acceptance requirements for E12-10-003 were also done. The spectrometers angular and momentum acceptance requirements were estimated using SIMC to simulate the D(e,e'p)n reaction at the same reaction kinematics described previously. The angular acceptances are measured from the target and measure the angular coverage of the spectrometers in the dispersive ( $\theta$ ) and non-dispersive ( $\phi$ ) planes. The momentum acceptance is defined as  $\delta = \frac{P - P_0}{P_0}$ , where  $P_0$  is the central momentum of the spectrometer. The results are shown for momentum acceptance correlations only in Figure 12

The results show correlated events between the HMS and SHMS for missing momentum setting of 0.5 GeV/c. The simulated events occupy a small part of the SHMS full acceptance as opposed to a wider range in the HMS

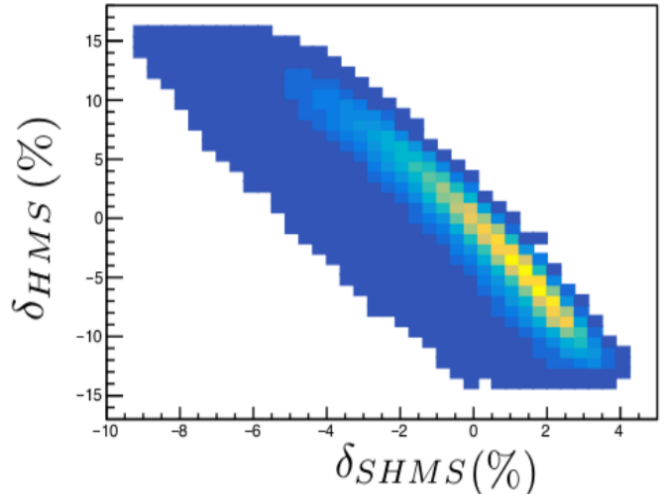


**Figure 12:** Momentum acceptance correlation.

acceptance. This effect becomes evident in the momentum acceptance, where the events occupy  $\sim -13$  to  $10\%$  of the HMS acceptance, but only  $\sim -4$  to  $4\%$  of the SHMS acceptance. For comparison, the spectrometers full acceptance parameters are shown in Table 6.

| Acceptance Parameter                | HMS       | SHMS      |
|-------------------------------------|-----------|-----------|
| Horizontal Acceptance $\phi$ (mrad) | $\pm 90$  | $\pm 60$  |
| Vertical Acceptance $\theta$ (mrad) | $\pm 100$ | $\pm 50$  |
| Momentum Acceptance (%)             | $\pm 15$  | (-10, 25) |

**Table 6:** Spectrometer Acceptance Parameters[4].

## 5 Summary

My proposed thesis subject will provide an opportunity to obtain new early D(e,e'p)n cross section measurements in an unexplored missing momentum region beyond 0.5 GeV/c at higher  $Q^2$  and kinematics were FSI and other processes (MEC and IC) are small. Considering that some kinematic quantities ( $\theta_e$ ,  $k_f$ , etc.) are not known to high precision during the commissioning phase, the systematics were shown to stay well below statistical uncertainties for the range of missing momentum being studied. Furthermore, a full understanding of the edges of the SHMS acceptance will not be required for the commissioning part, as demonstrated by the simulation results.

## References

- [1] BOEGLIN, W. U. Coincidence experiments with electrons. *Czechoslovak Journal of Physics* 45, 4/5 (1995), 296–335.
- [2] IBRAHIM, H. F. *The  $^2H(e,e'p)n$  Reaction at High Four Momentum Transfer*. PhD thesis, Norfolk, VA, 2006.
- [3] JONES, M. Private Communication, February 6, 2017.
- [4] JONES, M. Private Communication, January 15, 2017.
- [5] KHANAL, H. *Experimental Deuteron Momentum Distributions with Reduced Final State Interaction*. PhD thesis, Miami, FL, 2014.
- [6] LEO, W. *Techniques for Nuclear and Particle Physics Experiments: A How-to-Approach*. Springer-Verlag New York, LLC, New York, 1987.
- [7] ULMER, P., ET AL. Probing the high momentum component of the deuteron at high  $q^2$ . *Physics Review Letters* 89, 6 (2002).
- [8] WERNER U. BOEGLIN, M.K. JONES, K. A., ET AL. Deuteron Electro-Disintegration at Very High Missing Momenta. <http://arxiv.org/pdf/1410.6770.pdf>, October 2014. *Jefferson Lab Proposal E12-10-003*.
- [9] WERNER U. BOEGLIN, M. M. S. Modern Studies of the Deuteron: From the Lab Frame to the Light Front. *International Journal of Modern Physics E* 24 (2015), 24.
- [10] WERNER U. BOEGLIN, M.K. JONES, P. U., ET AL. Short-Distance Structure of the Deuteron and Reaction Dynamics in  $^2H(e,e'p)n$ . [https://www.jlab.org/exp\\_prog/proposals/01/PR01-020.pdf](https://www.jlab.org/exp_prog/proposals/01/PR01-020.pdf), 2001. *Jefferson Lab Proposal E01-020*.